Antarct. Meteorite Res., **19**, 58–78, 2006

Noble gases in solar-gas-rich and solar-gas-free polymict breccias

Takahito Osawa[1,2*] and Keisuke Nagao[2]

[1]*Research Group for Analytical Science, Japan Atomic Energy Agency (JAEA), Tokai-mura, Ibaraki 319-1195*
[2]*Laboratory for Earthquake Chemistry, Graduate School of Science, The University of Tokyo, Hongo, Tokyo 113-0033*
[*]*Corresponding author. E-mail: osawa.takahito@jaea.go.jp*

(Received August 25, 2005; Accepted January 18, 2006)

Abstract: Polymict breccias are useful for research of solar activity because some preserve plenty of solar noble gases implanted during asteroidal formation processes. In this study, noble gas compositions of Antarctic and non-Antarctic polymict breccias were determined using laser gas-extraction and stepwise pyrolysis techniques. Of the polymict breccias measured in this work, 5 of 18 were identified as gas-rich meteorites (regolith breccias) and 4 of those 5 are H chondrites. The high population of gas-rich H chondrites compared with L and LL chondrites was presumably related to the depth of regolith formed on each parent body. It is notable that the major part of polymict breccias did not have solar noble gases. Noble gas analyses with stepwise heating method were done for 11 polymict breccias. Gas-rich meteorites have high concentrations of solar-derived He and Ne, which were released at relatively low temperature steps. Cosmogenic nuclides were comparatively dominant at high temperature steps. Five sources determined the observed Ar isotopic compositions. The components were: atmospheric, radiogenic, solar wind (SW), solar energetic particles (SEP), and cosmogenic. In contrast, Ne isotopic compositions of most regolith breccias can be explained simply by three-component mixing, such as SW, SEP, and cosmogenic. Indications of primordial trapped components were observed only in Willard (b), in which carbonaceous chondrite clasts were discovered previously. Cosmic-ray exposure ages were calculated from excess ^{3}He, ^{21}Ne, and ^{38}Ar. Regolith breccias did not have systematically longer ages than gas-poor samples, indicating that the parent body exposure ages of the meteorites on the order of tens of millions of years at most.

key words: polymict breccia, noble gas, solar wind, SEP, ordinary chondrite

1. Introduction

Polymict breccias are stony meteorites that include clasts of different meteorite groups or petrologic types. Brecciated meteorites are formed by gardening on asteroidal parent bodies (Housen *et al*., 1979). They are the product of successive mechanical comminution, playing an important role for the evolution of asteroidal parent regoliths.

Some polymict breccias contain abundant solar-derived noble gases; they are called gas-rich meteorites, reflecting their irradiation history of accelerated solar particles on the parent bodies. Gerling and Levskii (1956) first reported extremely high concentra-

tions of noble gases in Pesyanoe aubrite; other gas-rich meteorites were discovered subsequently (*e.g.* Manuel and Kuroda, 1964). Gas-rich meteorites apart from the carbonaceous chondrite group generally have a dark-light structure (Goswami *et al*., 1984). The solar noble gases are generally trapped in the dark matrix contrasting with the light inclusions, indicating that the materials that composed the dark matrix existed on the surface of the parent body and were irradiated by the solar wind. Cosmogenic products are predominant in the light inclusions. However, the prominent structure is not observed in some gas-rich meteorites belonging to ordinary chondrite groups, for example Yamato-75029 (Nakashima *et al*., 2002).

Interplanetary dust particles (IDPs) and micrometeorites accreted on Earth are solar gas-rich extraterrestrial materials as well as gas-rich meteorites (Olinger *et al*., 1990; Pepin *et al*., 2000, 2001; Osawa and Nagao, 2002; Osawa *et al*., 2000, 2003a, b). The solar noble gases in the cosmic dust particles were recently implanted during their orbital evolution in interplanetary space. On the other hand, solar noble gases in some gas-rich meteorites may be fossils of ancient solar activity. For that reason, the noble gases in the gas-rich meteorites have been investigated to understand early solar activity (*e.g*., Padia and Rao, 1989; Rao *et al*., 1997). Moreover, the study of gas-rich meteorites has another importance. Such meteorites reflect the formation of the fundamental noble gas inventory of the solar system because solar noble gases are most representative for the noble gases in the solar nebula: the sun constitutes 99.9% of the solar system mass. Each gas-rich meteorite contains several independent noble gas components, such as low-energy solar wind (SW), solar energetic particles (SEP), cosmogenic nuclides produced by galactic or solar cosmic rays, and primordial trapped components. Such noble gas compositions in the gas-rich meteorites were established through complex irradiation (Schultz *et al*., 1972). The present study undertook comprehensive noble gas examination of 18 Antarctic and non-Antarctic polymict breccias to clarify their exposure histories on the parent bodies.

2. Samples and analytical method

This study measured 18 brecciated meteorites (Table 1). Of them, 13 were Antarctic polymict breccias—H, L, and LL ordinary chondrites—that were provided from the National Institute of Polar Research (NIPR). All the Antarctic meteorites are classified into the most brecciated meteorites, describing as "4" in the degree of brecciation (Kojima and Imae, 1998; Kojima, 2001). Gladstone (stone) is an H4 gas-rich chondrite, whose bulk noble gas composition was previously reported in Miura and Nagao (1992). NWA869 and Sahara98222 are meteorites found in the desert; their relatively high petrologic types are 5 and 6, respectively. Willard (b) is a rare type of brecciated ordinary chondrite that contains small carbonaceous chondrite clasts, which were identified as CI chondrite (Inada and Nagao, 2003; Osawa *et al*., 2005). Only Yamato-791826 is a polymict eucrite, which is tentatively paired with Y-82210 because of its field occurrence (Kojima and Imae, 2000).

Nine of 18 meteorites were measured by laser heating (Table 2) and nine others plus two gas-rich ones among the laser-heated samples were investigated by stepwise heating. Noble gas compositions of small chips (13.3–162.7 μg) of nine Antarctic meteorites were

Table 1. Meteorite samples measured in this work.

Sample	Class	Regolith breccia
Asuka-87154	L3	
Asuka-87155	L3	
Asuka-87166	L3	
Asuka-87191	H4	yes
Asuka-87192	H4	
Asuka-87214	H5	yes
Asuka-87250	LL3	
Asuka-87289	H3	
Asuka-87341	H4	
Gladstone	H4	yes
NWA869	L5	yes
Sahara98222	L6	
Willard (b)	H3.5-3.6	yes
Yamato-74112	H5	
Yamato-790521	LL	
Yamato-791067	LL	
Yamato-791108	LL5,6	
Yamato-791826	Euc	

Table 2. Result of laser gas-extraction analysis of Antarctic polymict breccias.

Sample	Weight	^{4}He	^{20}Ne	^{36}Ar	^{40}Ar	^{84}Kr	^{132}Xe	^{3}He/^{4}He	^{20}Ne/^{22}Ne	^{21}Ne/^{22}Ne	^{40}Ar/^{36}Ar	^{38}Ar/^{36}Ar
	(μg)	10^{-9} cm^{3}STP/g						($\times 10^{-4}$)				
Asuka-87154 (L3)	44.9	1950	79	5.5	2790	0.13	0.024	517 ± 69	2.05 ± 0.15	0.755 ± 0.026	508 ± 11	0.452 ± 0.030
Asuka-87155 (L3)	13.3	1500	44	9.95	4040	0.36	0.127	865 ± 165	<1	0.983 ± 0.081	406 ± 17	0.297 ± 0.031
Asuka-87191 (H4)	13.3	904000	1930	76.5	72900	0.773	0.101	7.3 ± 0.1	7.60 ± 0.12	0.341 ± 0.015	953 ± 9	0.260 ± 0.010
Asuka-87192 (H4)	46.3	20200	159	10.9	24700	0.549	0.197	17 ± 2	3.95 ± 0.17	0.566 ± 0.019	2271 ± 58	0.298 ± 0.011
Asuka-87214 (H5)	14	44000	2010	61.2	5940	0.552	0.135	6.7 ± 1.0	9.87 ± 0.23	0.107 ± 0.007	97 ± 2	0.215 ± 0.009
Asuka-87250 (LL3)	37.2	13700	214	39.2	35700	0.236	0.088	156 ± 20	0.78 ± 0.05	0.831 ± 0.015	911 ± 6	0.617 ± 0.020
Asuka-87289 (H3)	17.6	n.d.	198	5.04	8800	0.158	0.034	n.d.	9.29 ± 0.36	0.062 ± 0.009	1744 ± 74	0.211 ± 0.041
Asuka-87341 (H4)	162.7	1120	19	2.02	11100	0.024	0.009	145 ± 19	1.63 ± 0.16	0.761 ± 0.025	5490 ± 96	0.285 ± 0.040
Yamato-791108 (LL5,6)	34.2	1250	86	5.63	8360	0.142	0.028	777 ± 116	2.40 ± 0.22	0.687 ± 0.026	1484 ± 51	0.319 ± 0.081

Blank corrections were carried out for all data.

measured using laser gas-extraction to estimate their bulk noble gas compositions roughly. The experimental procedure was similar to that for measurements for micrometeorites, which is detailed in Osawa *et al*. (2003b). Each sample was set in a Ta-made sample holder and heated for 2 min by irradiation of a Nd-YAG continuous wave laser. The output power was about 2.5–5.0 W. A heated sample was melted entirely and noble gases were extracted completely by laser irradiation. Two Ti-Zr getters purified the extracted gases. Noble gas isotopes were detected on a modified VG-5400 mass spectrometer (MS-III). After bulk analysis, we selected two of the Antarctic gas-rich meteorites (Asuka-87191 and Asuka-87214) for further investigations.

The 2 gas-rich meteorites and the other 9 meteorites were wrapped in aluminum foil and set in a glass sample holder above an extraction furnace. These samples were preheated at 150°C for one day to remove adsorbed atmospheric gases. Noble gases were extracted by stepwise heating technique at each temperature step for 20 min. Extracted

gases were purified by two heated Ti-Zr getters in an ultra-high vacuum purification line to remove reactive gases. We trapped Ar, Kr, and Xe in a liquid-nitrogen-cooled charcoal trap; He and Ne were analyzed on another modified VG-5400 mass spectrometer (MS-II). We trapped Kr and Xe in a cryogenically cooled trap at 100 K and only Ar was measured. The Kr and Xe were respectively released from the trap at 135 K and 220 K. Sensitivity and mass discrimination effects were calibrated using an atmospheric noble gas standard and a helium standard gas with $^{3}He/^{4}He = 1.71 \times 10^{-4}$. Neon mass interferences caused by $^{40}Ar^{++}$ and CO_2^{++} were corrected using experimentally determined $^{40}Ar^{++}/^{40}Ar^{+}$ and CO_2^{++}/CO_2^{+} ratios (Osawa, 2004). During Ne analysis, argon and carbon dioxide were removed using a liquid-nitrogen-cooled trap close to an ion source.

3. Results and discussion

3.1. Bulk noble gas compositions of Antarctic polymict breccias

Laser gas-extraction measurement provided preliminary noble gas data for nine Antarctic polymict breccias. The advantage of the laser extraction system is that noble gas composition can be determined for an extremely small sample because of the low blank level. This study uses only 13.3–162.7 μg of the meteorite chips, containing matrix and clast. Noble gas concentrations and isotopic compositions of the nine brecciated ordinary chondrites are listed in Table 2. It is remarkable that a large diversity of noble gas concentrations exists in samples even though all of them are polymict breccias. The dispersion may reflect the heterogeneity of these meteorites because of the small weights of these samples. Asuka-87191 and Asuka-87214 have high concentrations of He and Ne, and high $^{20}Ne/^{22}Ne$ ratios, indicating the presence of solar noble gases clearly. The peculiarly low $^{40}Ar/^{36}Ar$ ratio of 97 detected for Asuka-87214 (H5) might reflect the presence of solar-derived Ar. The two meteorites also have relatively low $^{3}He/^{4}He$ ratios ($7.3 \pm 0.1 \times 10^{-4}$ and $6.7 \pm 1.0 \times 10^{-4}$), indicating that the contribution of cosmogenic ^{3}He is low and that solar He is predominant. Therefore, the two meteorites are regolith breccias. Asuka-87192 (H4) also has relatively high ^{4}He concentration and relatively low $^{3}He/^{4}He$ ratio. It is curious that ^{4}He was not detectable in Asuka-87289 (H3) in spite of that meteorite's comparatively high ^{20}Ne concentration. Helium in this meteorite might be totally depleted by heating, but the cause is unclear. Cosmogenic nuclides are dominant in the other five chondrites: no signs of solar noble gases exist. This rough measurement suggests two possibilities: (1) solar noble gases are localized to specific portions of a polymict breccia and solar gas-rich fragments of Asuka-87191 and Asuka-87214 (H5) were accidentally selected; alternatively, (2) the variation of noble gas compositions among these breccias indicates that some polymict breccias are not regolith breccias. Although preliminary measurement is insufficient to judge perfectly whether or not breccias with no solar noble gases are regolith breccias, meteorites other than Asuka-87191 (H4) and 87214 (H5) should not be classified as regolith breccias because even solar-gas-poor portions of a regolith breccia have ^{4}He concentrations greater than 1×10^{-5} cm^{3}STP/g, as explained later. The measured samples of Asuka-87192 (H4) and 87250 (LL3) are sufficiently large, at 46.3 and 37.2 μg, respectively, to reduce the effect of heterogeneity. Therefore, they are not classified into gas-rich meteorites here

judging from their ^{4}He concentrations and noble gas isotopic ratios. The heterogeneity of noble gases in regolith breccias and the variety of noble gas compositions among polymict breccias will be discussed below.

Bulk noble gas compositions for 18 meteorites measured in this work (see Tables 2 and 3) are discussed here before details of noble gas compositions for each meteorite because it is necessary to distinguish gas-rich meteorites from gas-poor meteorites. Some of them are calculated from results of stepwise heating analyses (Table 3), whose results are described in the next section. Figure 1 shows He and Ne isotopic ratios and concentrations for the polymict breccias measured in this work. The compositions shown in this figure are bulk compositions. Some meteorites have high ^{20}Ne/^{22}Ne and

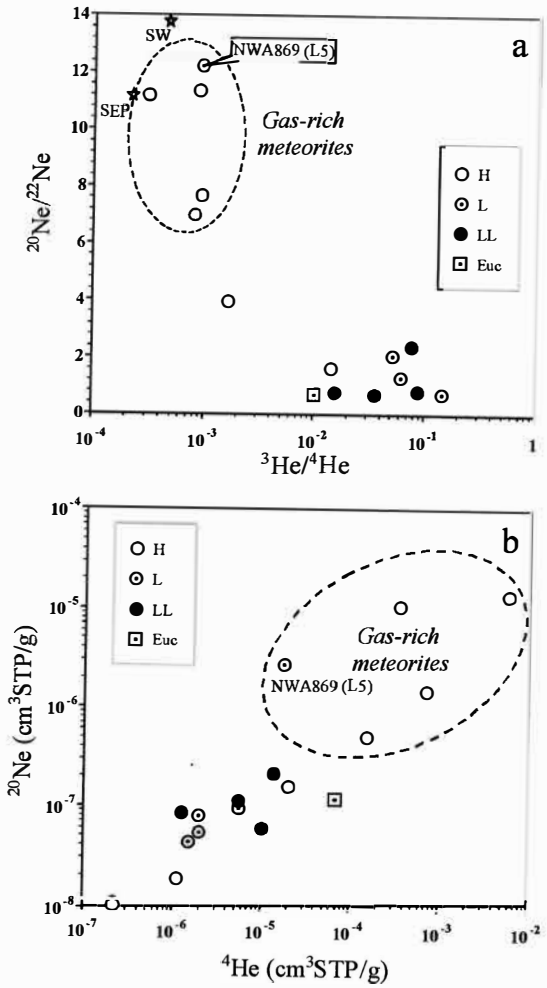

Fig. 1. Isotopic ratios (a) and concentrations (b) of He and Ne for bulk compositions of polymict breccias measured in this work. Five meteorites are classified into gas-rich meteorites and four of them are H chondrites. L and LL chondrites, except for NWA869 (L5), are solar-gas-free chondrites.

low $^{3}He/^{4}He$ ratios, indicating the presence of solar noble gases. We judged that the five meteorites (Asuka-87191, Asuka-87214, Willard (b), Gladstone, and NWA869) are gas-rich meteorites (*i.e.* regolith breccias), which have high ^{4}He and ^{20}Ne concentrations. It is remarkable that four of them are H chondrites and only one sample (NWA869) is an L chondrite. Although most L and LL chondrites are gas-poor meteorites, four of eight H brecciated chondrites have noble gases of solar origin. Asuka-87289 (H3) and Yamato-74112 (H5) are not regolith breccias: the former is not shown in the both figures because of lack of He data; the latter is not presented in the upper diagram because its Ne isotopic composition was not determined. The relatively high population of gas-rich H chondrites may not be accidental because most famous gas-rich ordinary chondrites are H chondrites, *e.g.*, Fayetteville (H4), Pantar (H5), Weston (H4), Noblesville (H4), Acfer 111 (H3-6), Tsukuba and so on (Merrihue *et al.*, 1962; Becker *et al.*, 1986; Becker and Pepin, 1991; Wieler *et al.*, 1989a; Lipschutz *et al.*, 1993; Pedroni and Begemann, 1994; Nakashima *et al.*, 2003). In addition, gas-rich L and LL chondrites are rare, for example, Hughes021 (L3) and Ghubara (L5) (Wieler *et al.*, 1999; Schultz and Franke, 2004). It is uncertain why the majority of gas-rich ordinary chondrites are H chondrites. It is clear, however, that many polymict H chondrites that have reached the Earth originated in materials that existed on the surface of their parent bodies during regolith formation. On the other hand, most polymict L and LL chondrites comprise materials that have never existed on surface portion and are shielded from solar irradiation, indicating that the meteorites formed in a relatively deep part of their parent bodies. The trend of the population of gas-rich meteorites might be related to the difference of regolith evolution of the respective parent bodies. The parent bodies of H chondrites produce more gas-rich meteorites than those of L and LL chondrites if the regolith layer on the parent bodies of H chondrites is systematically thicker than those of L and LL chondrites.

3.2. Stepwise heating for breccias

Table 3 presents a summary of results of noble gas measurements for 11 brecciated meteorites using stepwise heating technique. The two Asuka Antarctic breccias, Asuka-87191 (H4) and Asuka-87214 (H5), Willard (b) (H3.5–3.6) and Gladstone (H4) have very high noble gas concentrations. Release profiles of He and Ne for the four meteorites are shown in Fig. 2. Helium release profiles of Willard (b), Asuka-87191, and Asuka-87214 resemble one another: He gases are mainly released at the 600–800°C temperature range, revealing their similar exposure history on the parent body and in interplanetary space. However, noble gas concentrations in Willard (b) are considerably higher than in the Asuka meteorites. The He concentration in Willard (b) of 5.78×10^{-3} $cm^{3}STP/g$ is comparable with solar-gas-rich lunar meteorites, *e.g.* 5.83×10^{-3} $cm^{3}STP/g$ in QUE 93069 (Thalmann *et al.*, 1996). The Ne release patterns of Willard (b) and Asuka-87214 are remarkable: two peaks exist at 800–1000°C and 1100–1200°C in Willard (b) and at 600–1000°C and 1200–1400°C in Asuka-87214. The characteristic profile will be discussed later. Gladstone has a distinctive release profile, although the meteorite is also classified as an H chondrite. The main release temperatures of He and Ne are 800–1000°C and 1000–1200°C, which are higher than those of the other meteorites, indicating that solar-derived noble gases in Gladstone are in a more retentive site than in the other

Table 3. Noble gas compositions for polymict breccias.

Sample	Temp.	^{4}He	^{20}Ne	^{36}Ar	^{84}Kr	^{132}Xe	^{3}He/^{4}He ($\times 10^{-4}$)	^{20}Ne/^{22}Ne	^{21}Ne/^{22}Ne	^{40}Ar/^{36}Ar	^{38}Ar/^{36}Ar
	(°C)	(10^{-8} cm^{3}STP/g)									
Asuka-87191 (H4)	400	3,960	5.6	0.3	0.008	0.004	4.23 ± 0.04	12.01 ± 0.15	0.075 ± 0.002	325 ± 3	0.193 ± 0.002
(31.3 mg)	600	105,000	23	1.3	0.01	0.007	4.12 ± 0.02	10.85 ± 0.08	0.147 ± 0.004	633 ± 6	0.199 ± 0.001
	800	467,000	222	14	0.017	0.008	6.98 ± 0.06	9.213 ± 0.04	0.244 ± 0.004	1246 ± 6	0.235 ± 0.001
	1000	125,000	577	11	0.027	0.01	12 ± 0.1	8.801 ± 0.02	0.292 ± 0.003	1028 ± 4	0.282 ± 0.001
	1200	7,120	469	17	0.041	0.021	52.3 ± 0.2	7.523 ± 0.01	0.373 ± 0.006	190.9 ± 0.4	0.295 ± 0.001
	1400	135	154	13	0.047	0.039	431 ± 33	4.071 ± 0.01	0.645 ± 0.006	170.5 ± 0.4	0.385 ± 0.001
	1600	39	31	7.9	0.045	0.048	1711 ± 456	1.81 ± 0.01	0.838 ± 0.008	143 ± 1	0.49 ± 0.001
	1800	6.4	0.8	0.4	0.005	0.002	8.18 ± 9.68	0.39 ± 0.2	0.95 ± 0.021	188 ± 6	0.306 ± 0.007
	total	708,260	1,482	64	0.2	0.14	8.07 ± 0.09	7 ± 0.04	0.423 ± 0.005	561 ± 2	0.319 ± 0.001
Asuka-87214 (H5)	400	4,580	9	0.8	0.033	0.015	7.78 ± 0.03	11.19 ± 0.03	0.122 ± 0.002	819 ± 7	0.194 ± 0.001
(64.1 mg)	600	7,970	7.2	0.3	0.003	0.002	6.76 ± 0.04	10.52 ± 0.04	0.155 ± 0.003	1997 ± 51	0.204 ± 0.002
	800	110,000	173	12	0.022	0.009	7.74 ± 0.04	10.78 ± 0.03	0.162 ± 0.002	2960 ± 52	0.218 ± 0.001
	1000	26,500	172	6	0.016	0.011	13.01 ± 0.06	8.7 ± 0.01	0.281 ± 0.003	1065 ± 4	0.246 ± 0.001
	1200	1,817	50	2.2	0.007	0.005	37.2 ± 0.3	7.8 ± 0.02	0.331 ± 0.003	478 ± 1	0.299 ± 0.001
	1400	546	89	8.2	0.036	0.04	87.4 ± 1	5.34 ± 0.01	0.536 ± 0.005	298 ± 1	0.304 ± 0
	1600	13	11	3.4	0.03	0.035	599 ± 229	1.89 ± 0.01	0.845 ± 0.009	182 ± 0	0.317 ± 0.001
	1800	1.3	0.5	0.3	0.004	0.002	2.4 ± 15.5	1.1 ± 0.15	0.902 ± 0.02	212 ± 2	0.245 ± 0.002
	total	151,427	511	33	0.151	0.119	9.3 ± 0.07	7.66 ± 0.02	0.373 ± 0.004	1416 ± 20	0.26 ± 0.001
Asuka-87166 (L3)	600	93	11	0.6	0.028	0.011	614 ± 19	8.34 ± 0.16	0.155 ± 0.004	295 ± 2	0.193 ± 0.001
(30.7 mg)	1200	1,800	20	12	0.068	0.131	614 ± 4	1.12 ± 0.03	0.88 ± 0.008	224 ± 0.5	0.262 ± 0.003
	1800	86	24	16	0.124	0.236	766 ± 39	1.08 ± 0.03	0.918 ± 0.008	77.8 ± 0.3	0.275 ± 0.002
	total	1,980	54	29	0.219	0.378	620 ± 6	1.32 ± 0.04	0.878 ± 0.008	144.1 ± 0.4	0.268 ± 0.002
Yamato-74112 (H5)	600	28	0.4	0.3	0.027	0.019	897 ± 102	0.54 ± 0.69	0.748 ± 0.053	278 ± 3	0.201 ± 0.002
(27.3 mg)	1200	169	3.4	0.9	0.016	0.022	2113 ± 119	n.d.	0.987 ± 0.024	384 ± 3	0.812 ± 0.013
	1800	23	6.7	6.1	0.053	0.088	870 ± 188	0.31 ± 0.12	0.971 ± 0.014	138 ± 1	0.3358 ± 0.0009
	total	220	10.5	7.4	0.095	0.129	1828 ± 124	174.4 ± 1	0.389 ± 0.003		
Yamato-790521 (LL)	600	42	7.4	13	0.337	0.034	1003 ± 61	8.31 ± 0.08	0.145 ± 0.003	299 ± 1	0.1883 ± 0.0003
(34.2 mg)	1200	5,090	46	4.9	0.068	0.056	875 ± 4	0.79 ± 0.01	0.919 ± 0.008	613 ± 6	0.459 ± 0.002
	1800	374	60	15	0.087	0.105	990 ± 11	0.79 ± 0.01	0.939 ± 0.008	230 ± 1	0.713 ± 0.002
	total	5,506	113	33	0.491	0.195	884 ± 5	0.84 ± 0.01	0.925 ± 0.008	314.6 ± 1.5	0.466 ± 0.001
Yamato-791826 (Euc)	600	3,570	25	0.3	0.006	0.004	170 ± 1	0.65 ± 0.01	0.755 ± 0.006	352 ± 3	1.15 ± 0.02
(28.6 mg)	1200	63,700	78	47	0.085	0.042	98.7 ± 0.5	0.7 ± 0	0.853 ± 0.007	517 ± 4	1.43 ± 0.008
	1800	544	17	19	0.06	0.02	97.7 ± 1	0.6 ± 0	0.909 ± 0.009	272 ± 1	1.477 ± 0.004
	total	67,814	120	66	0.151	0.067	102 ± 1	0.71 ± 0.02	0.84 ± 0.007	445.7 ± 2.8	1.442 ± 0.007
Yamato-791067 (LL)	600	3,720	2.1	6.3	0.072	0.016	342 ± 2	0.42 ± 0.1	0.908 ± 0.012	3059 ± 203	0.282 ± 0.005
(32.1 mg)	1200	5,970	23	8.2	0.065	0.016	374 ± 2	0.69 ± 0.03	0.877 ± 0.008	2786 ± 167	0.438 ± 0.014
	1800	211	35	7.7	0.039	0.051	404 ± 8	0.73 ± 0.02	0.879 ± 0.007	721 ± 7	0.939 ± 0.009
	total	9,901	60	22	0.175	0.084	363 ± 2	0.7 ± 0.03	0.88 ± 0.008	2150.9 ± 122.3	0.566 ± 0.01
NWA869 (L5)	600	250	6.6	0.7	0.023	0.009	37 ± 0.5	12.1 ± 0.1	0.083 ± 0.003	1514 ± 41	0.193 ± 0.001
(32.4 mg)	1200	16,600	2,338	52	0.17	0.088	8.72 ± 0.05	12.52 ± 0.03	0.051 ± 0	771 ± 9	0.191 ± 0.0006
	1800	361	428	49	0.173	0.181	14.3 ± 0.2	10.85 ± 0.02	0.132 ± 0.001	102.7 ± 0.4	0.1961 ± 0.0004
	total	17,211	2,773	102	0.367	0.278	9.2 ± 0.1	12.23 ± 0.03	0.065 ± 0.001	455.6 ± 5.3	0.193 ± 0.001
Sahara98222 (L6)	600	1,220	3.8	51	2.451	0.209	1344 ± 9	1.05 ± 0.072	0.858 ± 0.01	314.7 ± 1	0.1913 ± 0.0002
(23.4mg)	1200	3,930	36	8.4	0.151	0.109	848 ± 4	0.708 ± 0.025	0.894 ± 0.008	2553 ± 129	0.537 ± 0.019
	1800	384	56	10	0.126	0.089	7964 ± 124	0.75 ± 0.016	0.905 ± 0.008	1164 ± 21	0.914 ± 0.013
	total	5,534	95	70	2.727	0.407	1451 ± 14	0.74 ± 0.02	0.899 ± 0.008	706.9 ± 19.5	0.336 ± 0.004
Willard (b) (H3.5-3.6)	400	65	0.06	0.01	0.0004	0.0002	2.75 ± 0.23	15.0 ± 3.2	n.d.	265 ± 95	0.200 ± 0.039
(27.0 mg)	500	55,857	72	3.5	0.054	0.048	3.23 ± 0.02	12.07 ± 0.04	0.036 ± 0.001	83.8 ± 0.3	0.1879 ± 0.0005
	600	1,205,000	516	23	0.06	0.063	2.72 ± 0.01	12.13 ± 0.08	0.042 ± 0.002	115.7 ± 0.2	0.1858 ± 0.0003
	700	1,601,000	960	41	0.069	0.052	2.9 ± 0.02	11.91 ± 0.06	0.041 ± 0.001	332 ± 1	0.1928 ± 0.0003
	800	1,374,000	1,780	29	0.052	0.033	3.1 ± 0.02	11.73 ± 0.03	0.042 ± 0.001	519 ± 3	0.2027 ± 0.0003
	900	941,000	2,440	25	0.058	0.049	3.24 ± 0.02	11.51 ± 0.03	0.047 ± 0.001	253 ± 1	0.2021 ± 0.0005
	1000	518,000	3,560	70	0.08	0.057	3.25 ± 0.02	11.42 ± 0.02	0.0442 ± 0.0004	18.34 ± 0.04	0.2017 ± 0.0004
	1100	69,600	1,160	24	0.037	0.031	4.13 ± 0.02	11.07 ± 0.03	0.048 ± 0.0005	31.7 ± 0.1	0.2119 ± 0.0004
	1200	13,700	1,950	70	0.1	0.074	6.14 ± 0.03	10.78 ± 0.02	0.0565 ± 0.0005	29.2 ± 0.1	0.2098 ± 0.0003
	1300	740	779	48	0.127	0.161	26 ± 0.2	10.26 ± 0.02	0.086 ± 0.001	9.84 ± 0.04	0.2097 ± 0.0003
	1400	137	391	22	0.06	0.082	74.5 ± 2.7	9.51 ± 0.02	0.123 ± 0.001	7.3 ± 0.1	0.2116 ± 0.0004
	1600	42	221	42	0.043	0.056	101 ± 12	8.56 ± 0.02	0.194 ± 0.002	8.72 ± 0.04	0.2173 ± 0.0004
	1800	29	6.3	3.7	0.017	0.016	0.76 ± 1.12	6.93 ± 0.05	0.312 ± 0.006	24.5 ± 0.4	0.2183 ± 0.0005
	total	5,779,170	13,835	401	0.759	0.723	3.03 ± 0.02	11.21 ± 0.03	0.055 ± 0.001	107.2 ± 0.4	0.2052 ± 0.0004
Gladstone (H4)	600	7,840	33	0.8	0.024	0.008	13.1 ± 0.4	11.33 ± 0.1	0.111 ± 0.002	519 ± 2	0.198 ± 0.001
(60.8 mg)	800	67,300	261	14	0.133	0.083	8.67 ± 0.03	11.63 ± 0.11	0.112 ± 0.002	2428 ± 12	0.226 ± 0.002
	1000	155,000	1,800	37	0.138	0.117	7.7 ± 0.1	12.49 ± 0.24	0.092 ± 0.001	996 ± 4	0.226 ± 0.001
	1200	104,000	3,660	41	0.035	0.019	6.8 ± 0.2	11.65 ± 0.1	0.0793 ± 0.0003	62.1 ± 0.3	0.209 ± 0.001
	1400	13,100	3,030	76	0.048	0.013	19.2 ± 0.5	11.36 ± 0.02	0.065 ± 0.001	21.1 ± 0.1	0.2145 ± 0.0003
	1600	616	1,730	116	0.127	0.058	136 ± 5	10.26 ± 0.01	0.123 ± 0.002	8.96 ± 0.11	0.2147 ± 0.0003
	1800	128	191	31	0.05	0.031	695 ± 9	7.27 ± 0.01	0.357 ± 0.005	9.32 ± 0.41	0.24 ± 0.001
	total	347,984	10,705	315	0.555	0.33	8.65 ± 0.12	11.33 ± 0.08	0.094 ± 0.001	244 ± 1	0.218 ± 0.001
Gladstone (1.12 g)[1]		210,000	5,690	335.4	0.425	0.383	8.27 ± 0.08	10.92 ± 0.03	0.1053 ± 0.0023	136.56 ± 0.35	0.2129 ± 0.002

All errors are one sigma.

Blank corrections were carried out for all data.

1) Miura and Nagao (1992).

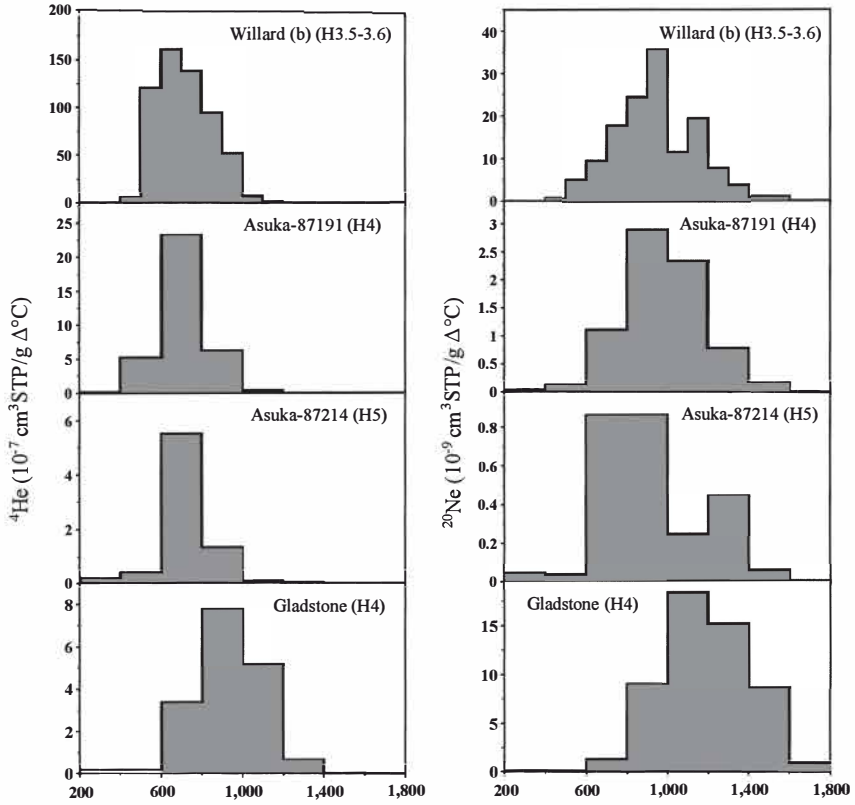

Fig. 2. Release profiles of ^{4}He and ^{20}Ne of four regolith breccias. The amounts of extracted gas per temperature interval are shown in these figures. Therefore, the areas of bars correspond with released amount of noble gases at each fraction. A characteristic double peak profile is found in Ne release patterns of Willard (b) and Asuka-87214.

meteorites. Gladstone has considerably higher concentrations of ^{20}Ne and ^{36}Ar than the Asuka meteorites. The ^{4}He, ^{20}Ne, and ^{36}Ar in Gladstone are released at higher temperatures than in the other three meteorites. Yamato-74112 (H5) has very low noble gas concentrations (Table 3), which are comparable with those of typical H5 chondrites with no solar gases. This meteorite apparently has no solar noble gases judging from its noble gas concentrations and isotopic compositions. Asuka-87166 (L3), Yamato-791067 (LL), Yamato-790521 (LL), and Sahara98222 (L6) are also not regolith breccias and cosmogenic nuclides are dominant. No sign of solar-derived noble gases is apparent in a polymict eucrite Yamato-791826, as is the case with other typical polymict eucrites. Nagao and Ogata (1989) measured three polymict eucrites; no sign of solar gases was found in them. Noble gas concentrations and He and Ne isotopic compositions of NWA869 prove that the meteorite should be classified into a regolith breccia. Large amounts of Ne are released at the 1200°C temperature step and bulk ^{20}Ne concentration of 2.77×10^{-6} cm^{3}STP/g is higher than for the two Asuka regolith breccias.

Profiles of ^{3}He/^{4}He ratios for four regolith breccias are shown in Fig. 3. A similar

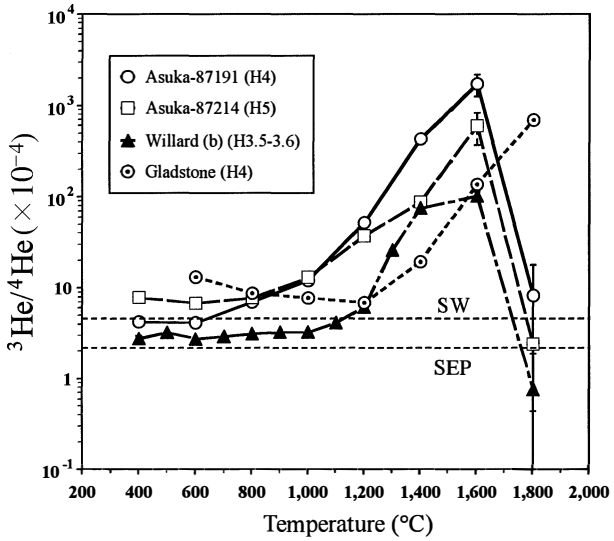

Fig. 3. *^{3}He/^{4}He ratios in each temperature step for four regolith breccias. Errors are one sigma. Dotted lines indicate the isotopic ratio of SW (4.57×10^{-4}; Benkert et al., 1993) and SEP (2.17×10^{-4}; Benkert et al., 1993). Solar-like isotopic ratios are observed at lower temperature steps. The maximum isotopic ratios are detected at 1600°C step in the two Asuka breccias and Willard (b), whereas Gladstone preserves cosmogenic He at 1800°C. A stable ^{3}He/^{4}He ratio observed in low temperature fractions of Willard (b) might directly reflect the composition of ancient solar ion flow.*

trend exists in the profiles of Asuka-87191, Asuka-87214 and Willard (b): the He isotopic ratio retains a low value at 400–900°C; then it rises with temperatures of 1000–1600°C; it reaches its highest value at 1600°C, and then decreases rapidly at the 1800°C step because almost all trapped He in the meteorites has already been extracted at 1600°C and lower temperature steps. Maximum ^{3}He/^{4}He ratios over 10^{-2} are detected for the breccias at the 1600°C step. The ^{3}He/^{4}He ratios of 1800°C step have large uncertainties caused by low amounts of released He. Solar-He is usually extracted at lower temperature steps. Cosmogenic He is released at high temperature steps, showing that cosmogenic He is more tightly preserved in meteorite-forming materials than solar-He because cosmogenic He is produced within the mineral grains, whereas solar-He is implanted only in uppermost 30–100 nm. The lowest ^{3}He/^{4}He ratios of the Asuka breccias are found in the 600°C step, which are close to the value of SW of $4.57\pm0.08\times10^{-4}$ (Benkert *et al.*, 1993). In the case of Willard (b), ^{3}He/^{4}He ratios released at 400–1000°C steps remain constant between that of SW and SEP of $2.17\pm0.05\times10^{-4}$ (Benkert *et al.*, 1993), indicating that the contribution of SEP-He is dominant. The ratio reaches a peak at 1600°C, as in the case of the two Asuka meteorites. Gladstone has a characteristic release profile. Its ^{3}He/^{4}He ratio decreases gradually at 600–1200°C, then it reaches the lowest ratio of $6.80\pm0.19\times10^{-4}$ at the 1200°C step. Subsequently, it rises at 1200–1800°C. The highest ^{3}He/^{4}He ratio is detected at 1800°C fraction, showing that cosmogenic He was not extracted completely at the 1600°C step. A large amount

of He was released at the 1800°C step in contrast with Asuka meteorites and Willard (b). Therefore, the $^3He/^4He$ ratio is determined with small uncertainty. The temperature of 1200°C is too high to extract solar wind He. For that reason, the lowest $^3He/^4He$ ratio may not be derived from a solar, but from a primordial component or a mixture between solar and cosmogenic ^3He. The $^3He/^4He$ ratio at 1200°C step should be lower than 6.8×10^{-4} and approach the ratio of SEP-He or He-Q (1.59×10^{-4}, Wieler *et al*., 1992) if cosmogenic He is eliminated.

Because of the effect of cosmogenic ^3He and SW-He, SEP-like He is not observed in the two Asuka meteorites and Gladstone, but the $^3He/^4He$ ratio of $4.12\pm0.02\times10^{-4}$ found in Asuka-87191 at 600°C step may show the presence of SEP-He because the ratio is lower than SW. The He isotopic ratio detected in Willard (b) at low temperature steps presumably reflects the composition of the averaged solar ion flow because the meteorite has extremely high concentration of He and interference by cosmogenic ^3He and primordial trapped component are comparatively small. The SEP/(SEP+SW) ratio of about 0.7 is calculated from the constant $^3He/^4He$ ratio of 2.9×10^{-4}. The high constancy of $^3He/^4He$ ratio in the wide range of temperature steps observed in the meteorite may mean a highly leveled value of the ancient solar ion flow for a long irradiation time.

The Ne isotopic compositions for five gas-rich polymict breccias are shown in a three-isotope diagram (Figs. 4a and 4b). The Ne-isotopic compositions of the two Asuka meteorites shift linearly to cosmogenic-Ne with temperature increase. The data plots of both meteorites shift along almost the same line and the Ne isotopic compositions are explainable by a simple two-component-mixing model: solar and cosmogenic. The line starts from a composition between SEP and SW, indicating the presence of both SEP-Ne and SW-Ne, in stark contrast with the case of micrometeorites, which typically have only SEP-Ne due to preferential SW loss during atmospheric entry (Osawa and Nagao, 2002; Osawa *et al*., 2000, 2003b). The result clearly shows that micrometeorites are not fragments of gas-rich meteorites. A remarkable pattern is observed at 600–800°C of Asuka-87214: the $^{20}Ne/^{22}Ne$ ratio of 800°C step is higher than that of 600°C, indicating that SW-Ne is more efficiently extracted at 800°C than at 600°C, and that the 800°C step corresponds with the temperature fraction at which the largest amount of Ne is released (Fig. 2). Although the Ne isotopic composition of Gladstone also shows the presence of SEP and SW, its isotopic profile differs greatly from that of the Asuka meteorites. In the case of the Asuka meteorites, the lowest $^{21}Ne/^{22}Ne$ ratio is observed at the lowest temperature step of 400°C and the $^{21}Ne/^{22}Ne$ ratio gradually increases concomitant with temperature. Such a simple Ne isotopic transition is not evident for Gladstone. The Ne isotopic composition of Gladstone rotates from the 600°C to the 1400°C step in the Ne isotope diagram (Fig. 4a). More than three components clearly contribute to the complex release profile. The isotopic profile is related closely with ^{20}Ne release pattern shown in Fig. 2. The ^{20}Ne was extracted mainly at 1200°C and 1400°C; low $^{21}Ne/^{22}Ne$ ratios were detected at these steps. The result shows that a main source of Ne in Gladstone has a Ne isotopic composition between SEP and SW, which is similar to those of Asuka meteorites. If three Ne components are assumed to explain the Ne isotopic profile of Gladstone, cosmogenic-Ne with high $^{21}Ne/^{22}Ne$ ratio, SEP-dominant component, and a distinctive Ne component with high $^{20}Ne/^{22}Ne$

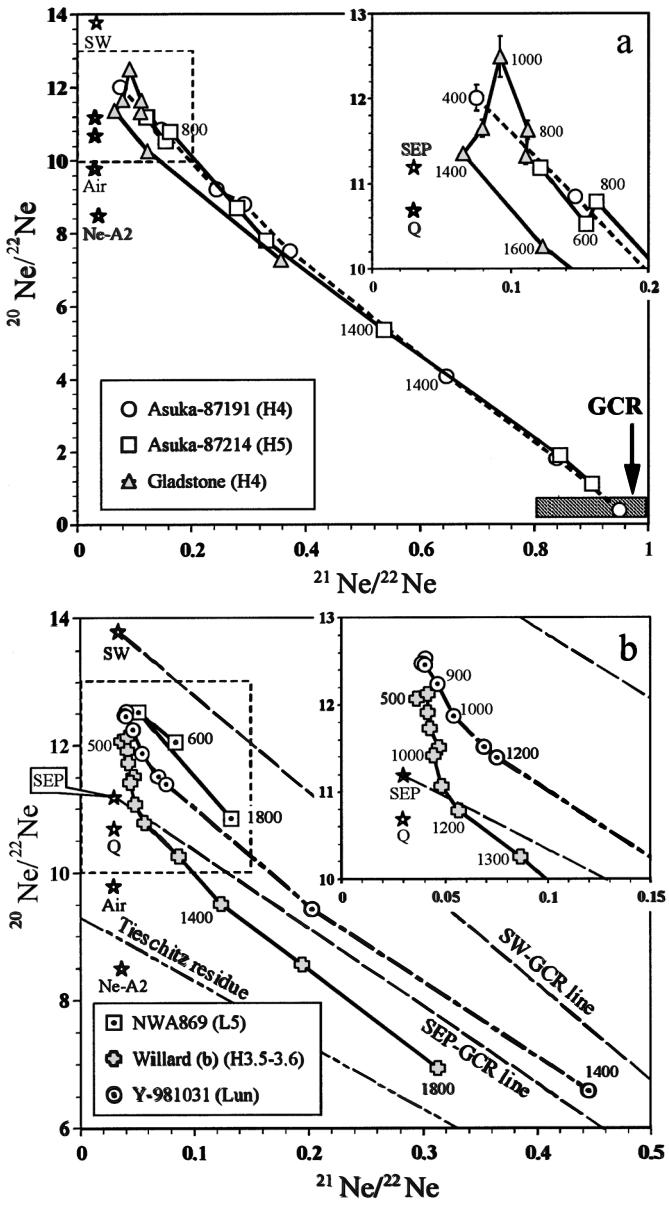

Fig. 4. A three-isotope plot of Ne. Upper right diagrams for each figure are magnified images of the dotted line squares. Numbers show temperatures in centigrade. Errors are one sigma. Y981031 data are according to Nagao and Okazaki (2002). SW and SEP-Ne data are of Benkert et al. (1993). Q-Ne data are of Wieler et al. (1992). Ne-A2 data are of Huss and Lewis (1994). Air-Ne data are of Eberhardt et al. (1965). A Tieschitz residue line is produced from data of Huss et al. (1996). The two Asuka meteorites have similar profiles: the respective Ne isotopic compositions shift linearly to a cosmogenic component (GCR shown here) concomitant with increased temperature. Gladstone has a complex profile. The profile of Willard (b) requires the contribution of a primordial trapped component.

ratio (*i.e.* SW-dominant component) are required. The SW-dominant component exists separately in the meteorite and the component is released mainly at the 1000°C step. However, that fact seems unusual: the SW component should be extracted at the lowest temperature step because of the low energy of SW. The most plausible explanation for that result is that solar noble gases are trapped in more than two individual phases with different release profiles.

Because Willard (b) has plenty of solar-derived Ne and the cosmogenic contribution is masked, the profile of the meteorite is more similar to that of lunar meteorites than to those of other regolith breccias, although $^{20}Ne/^{22}Ne$ ratio is systematically lower than that of a lunar meteorite Y981031 (Fig. 4b). The curved release profile of the lunar sample is explained simply by the different release temperatures of three Ne components: SW, SEP, and cosmogenic-Ne. That is, the order of extraction is SW, SEP, and cosmogenic. The release profile of Willard (b), however, cannot be explained by the mixing of the three components because Ne isotopic compositions released at 1200°C and higher steps are clearly affected by another component with a $^{20}Ne/^{22}Ne$ ratio that is lower than that of the SEP. The Ne isotopic compositions of the high temperature steps are distributed below the line of the SEP-GCR (galactic cosmic rays) mixing line and the compositions cannot be explained by the effect of cosmogenic Ne produced by the solar cosmic rays (SCR), which has lower $^{21}Ne/^{22}Ne$ than the GCR does. The result indicates that the meteorite has primordial trapped components (Q and Ne-A2) and the contributions by the pristine components are detectable at high temperature steps because solar-derived Ne have already been extracted at 1200°C or lower fractions. A regression line of HF/HCl treatment residues of Tieschitz (H3.6) made from data of Huss *et al.* (1996) is displayed in Fig. 4b for reference. Data plots of 1200–1800°C fractions are between the SEP-GCR line and the Tieschitz residue line, showing the presence of primordial Ne components, which are concentrated in the insoluble materials by hydrochloric and fluoric acids. Because the petrographic type of Willard (b) is 3.5–3.6 and this meteorite contains small carbonaceous chondrite clasts, the sign of primitive-Ne components is detectable. The contribution of primordial Ne can be estimated from a simple three-component mixing model: solar ($^{20}Ne/^{22}Ne=11.9$ and $^{21}Ne/^{22}Ne=0.030$), primordial ($^{20}Ne/^{22}Ne=8.72$ and $^{21}Ne/^{22}Ne=0.027$), and cosmogenic. The composition of solar-Ne (mixing of SW and SEP) is estimated from those of other gas-rich H meteorites. The primordial-Ne (composed of Q, HL, and E) is assumed by an average composition of CI chondrites, Ivuna (Black, 1972; Mazor *et al*., 1970). Nine percent of total ^{20}Ne (1.2×10^{-6} cm^{3}STP/g) is attributed to primordial Ne in the estimation and the concentration is significantly higher than those of the typical solar-gas-free H3.4, 3.5, and 3.6 chondrites ($<1\times10^{-7}$ cm^{3}STP/g.), showing the presence of carbonaceous chondrite clasts. However, the ^{20}Ne concentration is extremely high compared with CI chondrites of *ca.* 4×10^{-7} cm^{3}STP/g. Therefore, the concentration of primordial-Ne may be overestimated.

Solar-derived Ne is detectable in NWA869 (L5), but only three-step pyrolysis is conducted. The highest $^{20}Ne/^{22}Ne$ ratio (12.52 ± 0.03) among all data obtained in the present work was detected in the 1200°C step of the meteorite, showing the high SW/(SEP+SW) ratio of about 0.5, which is comparable with low temperature steps of lunar meteorites.

Two diagrams depicted in Fig. 5 are three-isotope plots of Ar; the Ar isotopic compositions of five gas-rich meteorites are presented there. Regarding the two Asuka meteorites, three sources mainly contribute to their Ar isotopic compositions: atmospheric, radiogenic, and cosmogenic Ar. This study does not identify SW and SEP-Ar.

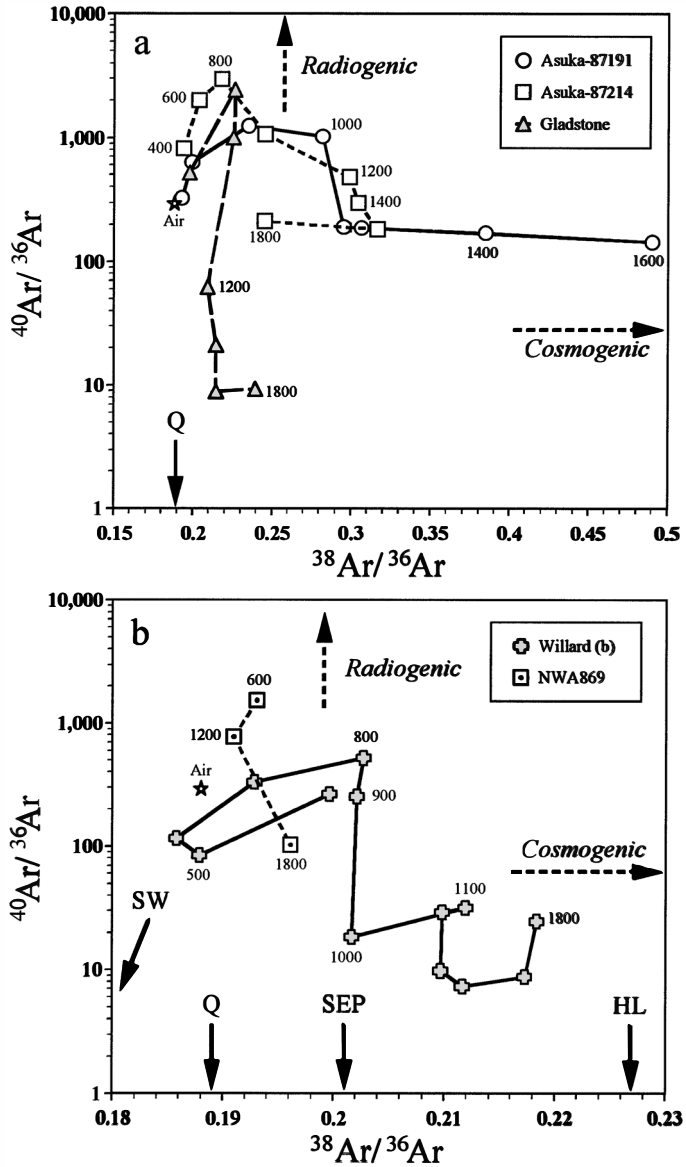

Fig. 5. Ar isotopic compositions of five regolith breccias. Errors are within the sizes of symbols. Air data is of Nier (1950). Numbers show temperatures in centigrade. High $^{40}Ar/^{36}Ar$ ratios caused by radiogenic ^{40}Ar produced from radioactive ^{40}K were observed at low temperatures of 600–1000°C. Several components are required to explain the complex profiles of Willard (b).

The existence of solar-Ar is also not verified in Gladstone, Willard (b), and NWA869. At the lowest temperature step, atmospheric Ar mainly controls their Ar compositions. From 400 to 800°C, the $^{40}Ar/^{36}Ar$ ratio increases because of radiogenic ^{40}Ar produced from ^{40}K. The highest $^{40}Ar/^{36}Ar$ ratio over 1000 was observed at 800°C in both Asuka meteorites. Radiogenic ^{40}Ar are extracted completely at 1000°C (Table 3). Therefore, cosmogenic Ar is dominant at 1200 to 1600°C steps. At the 1600°C step, the highest $^{38}Ar/^{36}Ar$ ratio was detected in both Asuka meteorites, being similar to the case of $^{3}He/^{4}He$ ratio. The Asuka meteorites have mutually similar Ar isotopic profiles; particularly, their modes of transition of $^{38}Ar/^{36}Ar$ ratios are analogous. Lower $^{40}Ar/^{36}Ar$ ratios than atmosphere detected at the high temperature steps might be derived from the trace of primordial trapped Ar components because solar-derived Ar will be extracted at lower temperature steps.

The profile of Ar isotopic composition of Gladstone differs distinctly from that of Asuka meteorites. It is strongly linked to ^{40}Ar and ^{36}Ar release patterns. After the release of radiogenic ^{40}Ar at 800°C and 1000°C steps, cosmogenic Ar does not perform a main role to control its Ar isotopic composition. From 1200°C to 1600°C steps, $^{40}Ar/^{36}Ar$ ratio drops suddenly because of the extremely large amount of released ^{36}Ar. The lowest $^{40}Ar/^{36}Ar$ ratio is 8.96 ± 0.11 detected at 1600°C step. The source of the large amount of ^{36}Ar is presumably Q-Ar. Indeed, the ^{36}Ar concentration of the meteorite (3.15×10^{-7} cm^{3}STP/g in total) corresponds with the range of typical non-gas-rich H4 chondrites, meaning that the contribution of solar-Ar is relatively low compared with the cases of He and Ne. However, the possibility of contribution of SEP-Ar cannot be ignored completely because SEP-Ne remains at the 1400°C step, as described previously, and the $^{38}Ar/^{36}Ar$ ratios of 1200, 1400, 1600°C steps are similar to that at SEP (0.196–0.206, Benkert *et al*., 1993). Nevertheless, the contribution of SEP-Ar should be low, even if SEP-Ar exists, because $^{20}Ne/^{36}Ar$ ratios of 1200–1600°C steps (24, 10, and 2) are lower than the SEP ratio of *ca.* 46 (Reams, 1998).

Willard (b) has an extremely complex release profile of Ar isotopes: the pattern is not similar to those of the Asuka meteorites and Gladstone (Fig. 5b). The convoluted pattern might be formed by contributions of several components: atmospheric, radiogenic, SW, SEP, cosmogenic, and Q-components. Presumably, the main source of ^{36}Ar is the primordial trapped component and solar-derived ^{36}Ar is comparatively minor because the bulk ^{36}Ar concentration of the meteorite of 4.01×10^{-7} cm^{3}STP/g corresponds with the range of normal H3 chondrites. However, the lowest $^{38}Ar/^{36}Ar$ ratio of 0.1858 ± 0.0003 observed at the 600°C step should be interpreted as a sign of SW-Ar because the ratio is evidently lower than that of the terrestrial atmosphere of 0.188 and the highest $^{20}Ne/^{22}Ne$ ratio is detected in the same fraction, indicating the presence of SW-Ne. A strange spiral pattern appearing in the high temperature steps might be affected by small CI chondrite fragments scattered throughout the meteorite (Osawa *et al*., 2005). The idea is supported by the presence of Ne-A2 in the meteorite, described previously, because the most abundant Ne component is Ne-A2, which accounts for about 60% of the total amount of ^{22}Ne. The Ar isotopic compositions of the steps higher than 1000°C are presumably controlled by the relative contributions of cosmogenic and primordial components of Q and HL.

3.3. *Irradiation history*

Cosmic-ray exposure ages of the polymict breccias can be calculated from excess ^{3}He, ^{21}Ne, and ^{38}Ar relative to solar isotopic ratio (Table 4). Production rates of typical meteorites are adopted here (Eugster, 1988; Eugster and Michel, 1995). The presence of solar noble gases in five gas-rich meteorites indicate that the meteorites were irradiated by solar wind on the surface of their parent bodies and were simultaneously exposed to galactic and solar cosmic rays. Therefore, gas-rich meteorites may systematically have longer exposure ages than gas-poor meteorites. Wieler *et al.* (1989a) reported that concentrations of solar and cosmogenic Ne in the Fayetteville (H4) matrix samples correlate, indicating simultaneous exposure of solar and cosmogenic. But such a trend is not observed here. The longest exposure age of 69 Ma is found in a solar-gas-poor breccia Asuka-87250 (LL3). Although Asuka-87191 (H4) (28 Ma in ^{21}Ne age) and Gladstone (H4) (20 Ma in ^{21}Ne age) have longer exposure ages than the main exposure age peak of H chondrites (*ca.* 7 Ma, Graf and Marti, 1995), H chondrites with 20–40 Ma exposure ages are not rare. Willard (b) has short exposure age (11 Ma in ^{21}Ne age) in spite of the highest concentration of solar noble gases. Exposure ages of other gas-rich meteorites previously reported calculated from cosmogenic ^{21}Ne are also widely distributed, for example, Acfer111 (H3–6) (29 Ma), Fayetteville (H4) (29 Ma), Noblesville (H4–6) (48 Ma), Pantar (H5) (3 Ma), Tysnesisland (H4) (8 Ma), Weston (H4) (44 Ma) (Pedroni and Begemann, 1994; Wieler *et al*., 1989a; Lipschutz *et al*., 1993; Signer and Suess, 1963; Schultz and Weber, 1996; Schultz *et al*., 1972). We cannot find clear trend in exposure age of gas-rich meteorites.

We conclude that 2π exposure ages of polymict breccias are the order of tens of millions of years at most, corresponding with the previous estimations (*e.g*., Wieler *et*

Table 4. Cosmic-ray exposure ages.

Sample	$^{3}He_{cos}$	$^{21}Ne_{cos}$	$^{38}Ar_{cos}$	T_3	T_{21}	T_{38}
	(10^{-9} cm^{3}STP/g)			Ma		
Asuka-87154 (L3)	101	29	1.7	6	9	4
Asuka-87155 (L3)	130	48	1.2	8	14	3
Asuka-87166 (L3)	123	36	2.7	8	11	6
Asuka-87191 (H4)	418	86	9.6	26	28	21
Asuka-87192 (H4)	29	22	1.4	2	7	3
Asuka-87214 (H5)	108	24	2.7	7	8	5
Asuka-87250 (LL3)	211	228	19.1	13	69	41
Asuka-87289 (H3)	n.d.	0.73	0.1	n.d.	0.2	0.3
Asuka-87341 (H4)	16	8.7	0.2	1	2	0.4
Gladstone (H4)	226	63	10.8	14	20	22
NWA869 (L5)	12	9	0.6	1	3	1
Sahara98222 (L6)	804	116	11.8	50	35	26
Willard (b) (H3.5-3.6)	n.d.[1)]	33	7.8	n.d.[1)]	11	16
Yamato-74112 (H5)	40	n.d.	1.7	3	n.d.	3
Yamato-790521 (LL)	486	125	10.4	30	38	22
Yamato-791067 (LL)	357	76	9.6	22	23	21
Yamato-791108 (LL5,6)	97	24	0.8	6	7	2
Yamato-791826 (Euc)	681	142	94.2	42	73	62

1) not determined due to the low ^{3}He/^{4}He ratio.

al., 1989b). Particularly, NWA869 (L5) has very short exposure age (3 Ma in ^{21}Ne age), although L chondrites generally have longer exposure age than H chondrites. Because the asteroid rotates, exposure time to the sun may be shorter than the cosmic-ray exposure on the parent body. Solar-derived noble gases in the gas-rich meteorite had been accumulated in a few million years or shorter. It is, however, very difficult to distinguish cosmogenic nuclides produced by regolith exposure from those by 4π exposure in interplanetary space. Surface exposure duration cannot be determined accurately and only the maximum age of parent exposure can be estimated roughly. If the relationship between the concentration of solar noble gases and exposure age is statistically discussed, more samples are required. However, the known gas-rich ordinary chondrites are not enough to obtain such the statistical data and it is necessary to discover more solar-gas-rich polymict breccias.

4. Conclusions

This study obtained several important findings from solar-gas-rich and solar-gas-free polymict breccias as summarized below.

Of 18 polymict breccias, 5 were identified as regolith breccias on the noble gas analyses and 4 of those were H chondrites, showing a biased population: four of eight H chondrites were gas-rich meteorites in contrast with a low population of gas-rich L and LL chondrites. Only one of nine was a gas-rich meteorite. It may be related to the difference of regolith evolution of parent bodies and H chondrite parent bodies are more frequently bombarded by meteorites, which originated in other asteroids. Indeed, carbonaceous chondrite clasts are frequently found in H chondrite regolith breccias and their mineralogical variations are similar with those of micrometeorites collected on the Earth (Noguchi *et al*., 2005). Major polymict breccias did not preserve solar noble gases, indicating that the solar-gas-free meteorites were formed in deep portion of parent bodies, or the duration of solar irradiation was extremely short due to frequent bombardment of meteorites. We found no trend of petrologic characteristics in regolith breccias, meaning that it was difficult to select gas-rich meteorites from a group of polymict breccias by their interior strictures. Indeed some gas-rich meteorites measured in the present work had no dark-light structures observed in famous gas-rich meteorites. Therefore, noble gas analyses using laser gas-extraction technique for small chips of polymict breccias are useful as a convenient test to discover gas-rich meteorites, although the method is not perfect because samples are small.

Stepwise heating measurements were performed for 11 meteorites. Solar-derived He and Ne were released at relatively low temperature steps and cosmogenic nuclides were predominant at high temperature steps. Their Ne isotopic compositions, apart from Willard (b), in which the presence of a primordial component was clearly observed, were interpreted as a simple three-component mix: SW, SEP, and cosmogenic.

Solar-gas-rich polymict breccias did not have systematically longer cosmic-ray exposure ages than solar-gas-free breccias, indicating the short parent exposure ages of several ten million years at most.

Acknowledgments

We thank the National Institute of Polar Research (NIPR) for providing Antarctic meteorites. We are grateful to R. Wieler and T. Nakamura for their constructive reviews.

References

Becker, R.H. and Pepin, R.O. (1991): Composition of solar wind noble gases released by surface oxidation of metal separate from the Weston meteorite. Earth Planet. Sci. Lett., **103**, 55–68.

Becker, R.H., Pepin, R.O., Rajan, R.S. and Rambaldi, E.R. (1986): Light noble gases in Weston metal grain surfaces. Meteoritics, **21**, 331–332 (abstract).

Benkert, J.P., Baur, H., Signer, P. and Wieler, R. (1993): He, Ne, and Ar from the solar wind and solar energetic particles in lunar ilmenites and pyroxenes. J. Geophys. Res., **98** (E7), 13147–13162.

Black, D.C. (1972): On the origins of trapped helium, neon and argon isotopic variations in meteorites-II. Carbonaceous meteorites. Geochim. Cosmochim. Acta, **36**, 377–394.

Eberhardt, P., Eugster, O. and Marti, K. (1965): A redetermination of the isotopic composition of atmospheric neon. Z. Naturforsch., **20a**, 623–624.

Eugster, O. (1988): Cosmic-ray rates for ^{3}He, ^{21}Ne, ^{38}Ar, ^{83}Kr and ^{126}Xe in chondrites based on ^{81}Kr-Kr exposure ages. Geochim. Cosmochim. Acta, **52**, 1649–1662.

Eugster, O. and Michel, T. (1995): Common asteroid break-up events of eucrites, diogenite, and howardites and cosmic ray production rates for noble gases in achondrites. Geochim. Cosmochim. Acta, **59**, 177–199.

Gerling, E.K. and Levskii, L.K. (1956): On the origin of the rare gases in stony meteorites. Dokl. Akad. Nauk SSSR, **110**, 750.

Goswami, J.N., Lal, D. and Wilkening, L.L. (1984): Gas-rich meteorites: Probes for particle environment and dynamical processes in the inner solar system. Space Sci. Rev., **37**, 111–159.

Graf, T. and Marti, K. (1995): Collisional history of H chondrites. J. Geophys. Res., **100**, 21247–21264.

Housen, K.R., Wilkening, L.L., Chapman, C.R. and Greenberg, R. (1979): Asteroidal regoliths. Icarus, **39**, 317–351.

Huss, G.R. and Lewis, R.S. (1994): Noble gases in presolar diamonds I: Three distinct components and their implication for diamond origins. Meteoritics, **29**, 791–810.

Huss, G.R., Lewis, R.S. and Hemkin, S. (1996): The "normal planetary" noble gas component in primitive chondrites: Compositions, carrier, and metamorphic history. Geochim. Cosmochim. Acta, **60**, 3311–3340.

Inada, A. and Nagao, K. (2003): Noble gases and cosmic-ray exposure history of Willard(b) H-chondrite: A breccia with carbonaceous chondritic inclusions. Meteorit. Planet. Sci., **38**, 5170 (abstract).

Kojima, H. (2001): Meteorite Newsletter, **10**.

Kojima, H. and Imae, N. (1998): Meteorite Newsletter, **7**.

Kojima, H. and Imae, N. (2000): Meteorite Newsletter, **9**.

Lipschutz, M.E. *et al.* (1993): Consortium study of the unusual H chondrite regolith breccia, Noblesville. Meteoritics, **28**, 528–537.

Manuel, O.K. and Kuroda, P.K. (1964): Isotopic composition of the rare gases in the Fayetteville meteorite. J. Geophys. Res., **7**, 1413–1419.

Mazor, E., Heymann, D. and Anders, E. (1970): Noble gases in carbonaceous chondrites. Geochim. Cosmochim. Acta, **34**, 781–824.

Merrihue, C.M., Pepin, R.O. and Reynolds, J.H. (1962): Rare gases in the chondrite Pantar. J. Geophys. Res., **67**, 2017–2021.

Miura, Y. and Nagao, K. (1992): Noble gases and ^{81}Kr-Kr exposure ages of non-Antarctic ordinary chondrites: An attempt to measure terrestrial ages of Antarctic meteorites. Proc. NIPR Symp. Antarct. Meteorites, **5**, 298–309.

Nagao, K. and Ogata, A. (1989): Noble gases and ^{81}Kr terrestrial ages of Antarctic eucrites. Mass Spectrosc.,

37, 313–324.
Nagao, K. and Okazaki, R. (2002): Noble gases of Yamato 981031 lunar meteorite. Antarctic Meteorites XXVII. Tokyo, Natl Inst. Polar Res., 107–109 (abstract).
Nakashima, D., Nakamura, T., Sekiya, M. and Takaoka, N. (2002): Cosmic-ray exposure age and heliocentric distance of the parent body of H chondrites Yamato-75029 and Tsukuba. Antarct. Meteorite Res., **15**, 97–113.
Nakashima, D., Nakamura, T. and Noguchi, T. (2003): Formation history of CI-like phyllosilicate-rich clasts in the Tsukuba meteorite inferred from mineralogy and noble gas signatures. Earth. Planet. Sci. Lett., **212**, 321–336.
Nier, A.O. (1950): A redetermination of the relative abundances of the isotopes of carbon, nitrogen, oxygen, argon and potassium. Phys. Rev., **77**, 789–793.
Noguchi, T., Nakamura, T., Nakashima, D., Inada, A., Nagao, K., Kusakabe, M. and Zolensky, M.E. (2005): Carbonaceous chondrite clasts in H chondrite regolith breccias: Dimmitt H4, Plainview H5, Tsukuba H4-5, Willard (b) H3.8, and Zag H3-6 meteorites. Astronomical Society of the Pacific Conference Series (in press)
Olinger, C.T., Maurette, M., Walker, R.M. and Hohenberg, C.M. (1990): Neon measurements of individual Greenland sediment particles: Proof of an extraterrestrial origin and comparison with EDX and morphological analyses. Earth Planet. Sci. Lett., **100**, 77–93.
Osawa, T. (2004): A new correction technique for mass interferences by $^{40}Ar^{++}$ and CO_2^{++} during isotope analysis of a small amount of Ne. J. Mass. Spectrom. Soc. Jpn., **52**, 230–232.
Osawa, T. and Nagao, K. (2002): Noble gas compositions of Antarctic micrometeorites collected at the Dome Fuji Station in 1996 and 1997. Meteorit. Planet. Sci., **37**, 911–936.
Osawa, T., Nagao K., Nakamura T. and Takaoka N. (2000): Noble gas measurement in individual micrometeorites using laser gas-extraction system. Antarct. Meteorite Res., **13**, 322–341.
Osawa, T., Nagao, K., Noguchi, T., Nakazawa, A. and Mikada, J.-I. (2003a): Remnant extraterrestrial noble gases in Antarctic cosmic spherules. Antarct. Meteorite Res., **16**, 196–219.
Osawa, T., Nakamura, T. and Nagao, K. (2003b): Noble gas isotopes and mineral assemblages of Antarctic micrometeorites collected at the meteorite ice field around the Yamato Mountains. Meteorit. Planet. Sci., **38**, 1627–1640.
Osawa, T., Kagi, H., Nakamura, T. and Noguchi, T. (2005): Infrared spectroscopic taxonomy for carbonaceous chondrites from speciation of hydrous components. Meteorit. Planet. Sci., **40**, 71–86.
Padia, J.T. and Rao, M.N. (1989): Neon isotope studies of Fayetteville and Kapoeta meteorites and clues to ancient solar activity. Geochim. Cosmochim. Acta, **53**, 1461–1467.
Pedroni, A. and Begemann, F. (1994): On unfractionated solar gases in the H3-6 meteorite Acfer 111. Meteoritics, **29**, 632–642.
Pepin, R.O., Palma, R.L. and Schlutter, D.J. (2000): Noble gases in interplanetary dust particles, I: The excess herium-3 problem and estimates of the relative fluxes of solar wind and solar energetic particles in interplanetary space. Meteorit. Planet. Sci., **35**, 495–504.
Pepin, R.O., Palma, R.L. and Schlutter, D.J. (2001): Noble gases in interplanetary dust particles, II: Excess helium-3 in cluster particles and modeling constraints on interplanetary dust particles exposures to cosmic-ray irradiation. Meteorit. Planet. Sci., **36**, 1515–1534.
Rao, M.N., Garrison, D.H., Palma, R.L. and Bogard, D.D. (1997): Energetic proton irradiation history of the howardite parent body regolith and implications for ancient solar activity. Meteorit. Planet. Sci., **32**, 531–543.
Reams, D.V. (1998): Solar energetic particles: Sampling coronal abundances. Space Sci. Rev., **85**, 327–340.
Schultz, L. and Franke, L. (2004): Helium, neon, and argon in meteorites: A data collection. Meteorit. Planet. Sci., **39**, 1889–1890.
Schultz, L. and Weber, H.W. (1996): Noble gases and H chondrite meteoroid streams: No confirmation. J. Geophys. Res., **101**, 21177–21181.
Schultz, L., Signer, P., Lorin, J.C. and Pellas, P. (1972): Complex irradiation history of the Weston chondrite. Earth Planet. Sci. Lett., **15**, 403–410.
Signer, P. and Suess, H. (1963): Rare gases in the sun, in the atmosphere, and in meteorites. Earth Science and Meteoritics, ed. by J. Geiss and E.D. Goldberg. Amsterdam, North-Holland, 241–272.

Thalmann, C., Eugster, O., Herzog, G.F., Klein, J., Krähenbühl, U., Vogt, S. and Xue, S. (1996): History of lunar meteorites Queen Alexandra Range 93069, Asuka 881757, and Yamato 793169 based on noble gas isotopic abundances, radionuclide concentrations, and chemical composition. Meteorit. Planet. Sci., **31**, 857–868.

Wieler, R., Baur, H., Pedroni, A., Signer, P. and Pellas, P. (1989a): Exposure history of the regolithic chondrite Fayetteville: I. Solar-gas-rich matrix. Geochim. Cosmochim. Acta, **53**, 1441–1448.

Wieler, R., Graf, Th., Pedroni, A., Signer, P., Pellas, P., Fieni, C., Suter, M., Vogt, S., Clayton, R.N. and Laul, J.C. (1989b): Exposure history of the regolithic chondrite Fayetteville. II. Solar-gas-free light inclusions. Geochim. Cosmochim. Acta, **53**, 1449–1459.

Wieler, R., Anders, E., Baur, H., Lewis, R.S. and Signer, P. (1992): Characterization of 29 Q-gases and other noble gas components in the Murchison meteorite. Geochim. Cosmochim. Acta, **56**, 2907–2921.

Wieler, R., Baur, H., Busemann, H., Heber, V.S. and Leya, I. (1999): Noble gases in desert meteorites: Howardites, unequilibrated chondrites, regolith breccias and an LL7. Workshop on Extraterrestrial Materials from Cold and Hot Deserts, ed. by L. Schultz *et al.* Houston, Lunar Planet. Inst., 90–94 (LPI Cont. 997).

Appendix. Kr and Xe isotopic compositions for polymict breccias.

Sample	Temp.	$^{78}Kr/^{84}Kr$	$^{80}Kr/^{84}Kr$	$^{82}Kr/^{84}Kr$	$^{83}Kr/^{84}Kr$	$^{86}Kr/^{84}Kr$	$^{124}Xe/^{132}Xe$
Asuka-87191	400	0.0066 ± 0.0014	0.0416 ± 0.0030	0.196 ± 0.009	0.200 ± 0.011	0.304 ± 0.014	0.0164 ± 0.0040
(31.3 mg)	600	0.0070 ± 0.0010	0.0445 ± 0.0016	0.205 ± 0.006	0.200 ± 0.007	0.308 ± 0.008	0.0092 ± 0.0024
	800	0.0089 ± 0.0011	0.0804 ± 0.0112	0.225 ± 0.014	0.209 ± 0.014	0.309 ± 0.016	0.0378 ± 0.0060
	1000	0.0099 ± 0.0004	0.0914 ± 0.0067	0.234 ± 0.012	0.231 ± 0.010	0.303 ± 0.010	0.0254 ± 0.0042
	1200	0.0085 ± 0.0012	0.0667 ± 0.0019	0.218 ± 0.006	0.219 ± 0.007	0.307 ± 0.004	0.0105 ± 0.0020
	1400	0.0092 ± 0.0002	0.0752 ± 0.0024	0.223 ± 0.003	0.219 ± 0.003	0.306 ± 0.003	0.0059 ± 0.0003
	1600	0.0085 ± 0.0004	0.0615 ± 0.0017	0.220 ± 0.003	0.215 ± 0.002	0.308 ± 0.004	0.0058 ± 0.0007
	1800	0.0063 ± 0.0007	0.0396 ± 0.0023	0.206 ± 0.006	0.204 ± 0.012	0.311 ± 0.014	0.0219 ± 0.0048
	total	0.0087 ± 0.0007	0.0692 ± 0.0034	0.221 ± 0.006	0.217 ± 0.006	0.307 ± 0.007	0.0106 ± 0.0016
Asuka-87214	400	0.0061 ± 0.0004	0.0418 ± 0.0011	0.204 ± 0.004	0.203 ± 0.003	0.305 ± 0.004	0.0053 ± 0.0006
(64.1 mg)	600	0.0073 ± 0.0016	0.0495 ± 0.0019	0.201 ± 0.007	0.204 ± 0.006	0.309 ± 0.006	0.0112 ± 0.0025
	800	0.0120 ± 0.0030	0.0721 ± 0.0129	0.215 ± 0.013	0.215 ± 0.012	0.313 ± 0.031	0.0800 ± 0.0230
	1000	0.0094 ± 0.0013	0.0762 ± 0.0072	0.227 ± 0.009	0.217 ± 0.013	0.301 ± 0.012	0.0156 ± 0.0040
	1200	0.0083 ± 0.0008	0.0897 ± 0.0036	0.223 ± 0.007	0.214 ± 0.005	0.312 ± 0.008	0.0093 ± 0.0018
	1400	0.0074 ± 0.0006	0.0651 ± 0.0013	0.217 ± 0.005	0.210 ± 0.005	0.309 ± 0.005	0.0063 ± 0.0009
	1600	0.0066 ± 0.0005	0.0431 ± 0.0008	0.206 ± 0.002	0.206 ± 0.003	0.310 ± 0.005	0.0053 ± 0.0004
	1800	0.0066 ± 0.0009	0.0399 ± 0.0020	0.203 ± 0.004	0.201 ± 0.006	0.306 ± 0.008	0.0127 ± 0.0038
	total	0.0079 ± 0.0010	0.0580 ± 0.0036	0.212 ± 0.006	0.209 ± 0.006	0.308 ± 0.009	0.0127 ± 0.0028
Asuka-87166	600	0.0053 ± 0.0008	0.0403 ± 0.0007	0.201 ± 0.003	0.201 ± 0.007	0.309 ± 0.005	0.0059 ± 0.0028
(30.7 mg)	1200	0.0070 ± 0.0003	0.0759 ± 0.0020	0.220 ± 0.003	0.212 ± 0.002	0.311 ± 0.004	0.0047 ± 0.0005
	1800	0.0068 ± 0.0004	0.0647 ± 0.0016	0.216 ± 0.003	0.209 ± 0.002	0.313 ± 0.003	0.0046 ± 0.0002
	total	0.0067 ± 0.0004	0.0651 ± 0.0016	0.215 ± 0.003	0.209 ± 0.003	0.312 ± 0.004	0.0047 ± 0.0004
Yamato-74112	600	0.0063 ± 0.0010	0.0390 ± 0.0025	0.201 ± 0.005	0.202 ± 0.004	0.309 ± 0.010	0.0038 ± 0.0006
(27.3 mg)	1200	0.0067 ± 0.2189	0.0493 ± 0.0031	0.209 ± 0.006	0.210 ± 0.003	0.309 ± 0.008	0.0045 ± 0.0016
	1800	0.0062 ± 0.0012	0.0424 ± 0.0014	0.206 ± 0.004	0.207 ± 0.002	0.314 ± 0.003	0.0045 ± 0.0008
	total	0.0063 ± 0.0368	0.0426 ± 0.0020	0.205 ± 0.004	0.206 ± 0.003	0.312 ± 0.006	0.0044 ± 0.0009
Yamato-790521	600	0.0059 ± 0.0001	0.0403 ± 0.0006	0.203 ± 0.002	0.202 ± 0.003	0.310 ± 0.003	0.0044 ± 0.0004
(34.2 mg)	1200	0.0074 ± 0.0008	0.0920 ± 0.0039	0.226 ± 0.003	0.214 ± 0.005	0.309 ± 0.005	0.0046 ± 0.0008
	1800	0.0099 ± 0.0007	0.1937 ± 0.0117	0.276 ± 0.006	0.231 ± 0.004	0.306 ± 0.005	0.0052 ± 0.0005
	total	0.0068 ± 0.0003	0.0745 ± 0.0030	0.219 ± 0.003	0.209 ± 0.003	0.309 ± 0.004	0.0049 ± 0.0006
Yamato-791826	600	0.0098 ± 0.0050	0.0550 ± 0.0046	0.223 ± 0.005	0.227 ± 0.010	0.308 ± 0.010	0.0077 ± 0.0069
(28.6 mg)	1200	0.0689 ± 0.0220	0.2256 ± 0.0419	0.440 ± 0.060	0.515 ± 0.067	0.259 ± 0.010	0.0366 ± 0.0105
	1800	0.0481 ± 0.0058	0.1632 ± 0.0131	0.373 ± 0.018	0.434 ± 0.026	0.268 ± 0.007	0.0601 ± 0.0074
	total	0.0583 ± 0.0149	0.1939 ± 0.0290	0.404 ± 0.041	0.471 ± 0.049	0.265 ± 0.009	0.0418 ± 0.0093
Yamato-791067	600	0.0081 ± 0.0023	0.0475 ± 0.0028	0.209 ± 0.008	0.213 ± 0.012	0.308 ± 0.013	0.0104 ± 0.0083
(32.1 mg)	1200	0.0119 ± 0.0031	0.0540 ± 0.0043	0.221 ± 0.003	0.219 ± 0.005	0.291 ± 0.011	0.0089 ± 0.0113
	1800	0.0132 ± 0.0026	0.0710 ± 0.0043	0.231 ± 0.006	0.233 ± 0.004	0.306 ± 0.008	0.0065 ± 0.0019
	total	0.0106 ± 0.0027	0.0551 ± 0.0037	0.218 ± 0.006	0.220 ± 0.008	0.302 ± 0.011	0.0077 ± 0.0050
NWA869	600	0.0060 ± 0.0017	0.0427 ± 0.0030	0.201 ± 0.003	0.201 ± 0.002	0.305 ± 0.008	0.0040 ± 0.0035
(32.4 mg)	1200	0.0064 ± 0.0048	0.0480 ± 0.0041	0.207 ± 0.009	0.202 ± 0.011	0.301 ± 0.007	0.0070 ± 0.0046
	1800	0.0063 ± 0.0004	0.0445 ± 0.0013	0.207 ± 0.003	0.204 ± 0.002	0.313 ± 0.003	0.0043 ± 0.0003
	total	0.0063 ± 0.0025	0.0460 ± 0.0027	0.207 ± 0.006	0.203 ± 0.006	0.307 ± 0.005	0.0051 ± 0.0018
Sahara98222	600	0.0060 ± 0.0003	0.0399 ± 0.0004	0.202 ± 0.002	0.201 ± 0.001	0.308 ± 0.002	0.0043 ± 0.0014
(23.4 mg)	1200	0.0074 ± 0.0025	0.0486 ± 0.0035	0.210 ± 0.004	0.212 ± 0.006	0.310 ± 0.012	0.0079 ± 0.0034
	1800	0.0089 ± 0.0027	0.0567 ± 0.0023	0.213 ± 0.006	0.219 ± 0.003	0.305 ± 0.004	0.0065 ± 0.0032
	total	0.0062 ± 0.0005	0.0412 ± 0.0007	0.203 ± 0.002	0.202 ± 0.001	0.308 ± 0.002	0.0057 ± 0.0023
Willard (b)	400	0.0101 ± 0.0270	0.0602 ± 0.0174	0.223 ± 0.079	0.215 ± 0.053	0.319 ± 0.069	0.0261 ± 0.0299
(27.0 mg)	500	0.0066 ± 0.0013	0.0392 ± 0.0009	0.201 ± 0.002	0.204 ± 0.003	0.305 ± 0.004	0.0036 ± 0.0011
	600	0.0057 ± 0.0024	0.0417 ± 0.0008	0.202 ± 0.003	0.202 ± 0.003	0.309 ± 0.004	0.0045 ± 0.0015
	700	0.0090 ± 0.0034	0.0446 ± 0.0019	0.205 ± 0.008	0.207 ± 0.009	0.317 ± 0.019	0.0065 ± 0.0049
	800	0.0085 ± 0.0014	0.0504 ± 0.0041	0.208 ± 0.008	0.208 ± 0.007	0.309 ± 0.006	0.0062 ± 0.0051
	900	0.0068 ± 0.0030	0.0481 ± 0.0038	0.205 ± 0.006	0.204 ± 0.008	0.310 ± 0.007	0.0039 ± 0.0013
	1000	0.0080 ± 0.0041	0.0428 ± 0.0008	0.199 ± 0.005	0.200 ± 0.006	0.312 ± 0.005	0.0071 ± 0.0011
	1100	0.0055 ± 0.0015	0.0429 ± 0.0020	0.205 ± 0.004	0.206 ± 0.004	0.315 ± 0.003	0.0047 ± 0.0014
	1200	0.0066 ± 0.0008	0.0434 ± 0.0009	0.206 ± 0.002	0.205 ± 0.002	0.316 ± 0.004	0.0049 ± 0.0013
	1300	0.0064 ± 0.0009	0.0403 ± 0.0012	0.204 ± 0.001	0.203 ± 0.002	0.315 ± 0.003	0.0042 ± 0.0008
	1400	0.0060 ± 0.0012	0.0395 ± 0.0013	0.202 ± 0.002	0.202 ± 0.004	0.315 ± 0.003	0.0045 ± 0.0006
	1600	0.0064 ± 0.0013	0.0403 ± 0.0013	0.202 ± 0.003	0.202 ± 0.003	0.317 ± 0.005	0.0041 ± 0.0008
	1800	0.0056 ± 0.0025	0.0409 ± 0.0033	0.200 ± 0.004	0.202 ± 0.004	0.312 ± 0.007	0.0040 ± 0.0016
	total	0.0069 ± 0.0019	0.0428 ± 0.0016	0.203 ± 0.004	0.204 ± 0.004	0.313 ± 0.006	0.0048 ± 0.0015
Gladstone	600	0.0057 ± 0.0005	0.0430 ± 0.0005	0.202 ± 0.003	0.203 ± 0.007	0.302 ± 0.003	0.0049 ± 0.0005
(60.8 mg)	800	0.0102 ± 0.0017	0.0542 ± 0.0019	0.208 ± 0.016	0.208 ± 0.018	0.309 ± 0.010	0.0143 ± 0.0023
	1000	0.0116 ± 0.0030	0.0646 ± 0.0049	0.223 ± 0.014	0.208 ± 0.007	0.307 ± 0.013	0.0123 ± 0.0010
	1200	0.0092 ± 0.0015	0.0586 ± 0.0037	0.209 ± 0.014	0.198 ± 0.014	0.316 ± 0.009	0.0097 ± 0.0035
	1400	0.0075 ± 0.0008	0.0550 ± 0.0029	0.209 ± 0.005	0.210 ± 0.003	0.306 ± 0.003	0.0061 ± 0.0009
	1600	0.0071 ± 0.0004	0.0457 ± 0.0015	0.206 ± 0.004	0.202 ± 0.003	0.306 ± 0.004	0.0045 ± 0.0005
	1800	0.0071 ± 0.0002	0.0453 ± 0.0015	0.204 ± 0.002	0.204 ± 0.004	0.309 ± 0.005	0.0044 ± 0.0002
	total	0.0091 ± 0.0014	0.0539 ± 0.0028	0.211 ± 0.010	0.206 ± 0.009	0.308 ± 0.008	0.0101 ± 0.0012

Errors are one sigma.
Blank corrections were carried out for all data.

Appendix (continued).

Sample	Temp.	$^{126}Xe/^{132}Xe$	$^{128}Xe/^{132}Xe$	$^{129}Xe/^{132}Xe$	$^{130}Xe/^{132}Xe$	$^{131}Xe/^{132}Xe$	$^{134}Xe/^{132}Xe$	$^{136}Xe/^{132}Xe$
Asuka-87191	400	0.0029 ± 0.0006	0.0731 ± 0.0052	1.023 ± 0.027	0.154 ± 0.006	0.797 ± 0.035	0.383 ± 0.012	0.326 ± 0.018
(31.3 mg)	600	0.0037 ± 0.0010	0.0748 ± 0.0050	1.026 ± 0.023	0.153 ± 0.005	0.797 ± 0.017	0.389 ± 0.016	0.330 ± 0.009
	800	0.0044 ± 0.0024	0.0769 ± 0.0099	1.150 ± 0.059	0.156 ± 0.014	0.807 ± 0.037	0.371 ± 0.023	0.333 ± 0.043
	1000	0.0056 ± 0.0013	0.0870 ± 0.0065	1.746 ± 0.045	0.160 ± 0.010	0.820 ± 0.037	0.380 ± 0.018	0.355 ± 0.022
	1200	0.0062 ± 0.0006	0.0867 ± 0.0076	1.518 ± 0.041	0.163 ± 0.006	0.838 ± 0.034	0.383 ± 0.007	0.328 ± 0.003
	1400	0.0048 ± 0.0003	0.0829 ± 0.0026	1.242 ± 0.008	0.163 ± 0.002	0.821 ± 0.012	0.385 ± 0.006	0.322 ± 0.004
	1600	0.0047 ± 0.0002	0.0834 ± 0.0014	1.245 ± 0.013	0.163 ± 0.003	0.825 ± 0.009	0.383 ± 0.005	0.321 ± 0.004
	1800	0.0041 ± 0.0019	0.0730 ± 0.0042	1.123 ± 0.045	0.156 ± 0.006	0.828 ± 0.047	0.396 ± 0.030	0.333 ± 0.019
	total	0.0049 ± 0.0006	0.0827 ± 0.0039	1.296 ± 0.022	0.161 ± 0.004	0.822 ± 0.019	0.383 ± 0.009	0.326 ± 0.009
Asuka-87214	400	0.0033 ± 0.0004	0.0725 ± 0.0012	1.031 ± 0.012	0.152 ± 0.003	0.794 ± 0.015	0.390 ± 0.004	0.329 ± 0.007
(64.1 mg)	600	0.0035 ± 0.0011	0.0705 ± 0.0033	1.075 ± 0.008	0.151 ± 0.009	0.791 ± 0.026	0.384 ± 0.010	0.329 ± 0.009
	800	0.0056 ± 0.0033	0.0817 ± 0.0060	1.405 ± 0.115	0.165 ± 0.013	0.800 ± 0.081	0.394 ± 0.018	0.291 ± 0.034
	1000	0.0051 ± 0.0009	0.0810 ± 0.0060	2.156 ± 0.089	0.160 ± 0.008	0.805 ± 0.027	0.389 ± 0.011	0.322 ± 0.017
	1200	0.0050 ± 0.0010	0.0813 ± 0.0026	2.373 ± 0.043	0.161 ± 0.005	0.808 ± 0.019	0.388 ± 0.007	0.336 ± 0.005
	1400	0.0046 ± 0.0004	0.0819 ± 0.0018	1.512 ± 0.020	0.160 ± 0.004	0.813 ± 0.012	0.386 ± 0.005	0.323 ± 0.005
	1600	0.0042 ± 0.0002	0.0831 ± 0.0011	1.357 ± 0.014	0.163 ± 0.002	0.822 ± 0.004	0.385 ± 0.003	0.325 ± 0.002
	1800	0.0039 ± 0.0005	0.0787 ± 0.0063	1.334 ± 0.034	0.158 ± 0.009	0.801 ± 0.021	0.377 ± 0.010	0.316 ± 0.010
	total	0.0044 ± 0.0006	0.0807 ± 0.0024	1.479 ± 0.032	0.160 ± 0.004	0.811 ± 0.017	0.387 ± 0.006	0.322 ± 0.008
Asuka-87166	600	0.0038 ± 0.0018	0.0707 ± 0.0023	1.047 ± 0.033	0.154 ± 0.004	0.793 ± 0.016	0.396 ± 0.008	0.334 ± 0.007
(30.7 mg)	1200	0.0043 ± 0.0008	0.0843 ± 0.0018	1.502 ± 0.018	0.161 ± 0.002	0.817 ± 0.006	0.385 ± 0.004	0.329 ± 0.006
	1800	0.0042 ± 0.0002	0.0845 ± 0.0016	1.507 ± 0.019	0.160 ± 0.002	0.811 ± 0.005	0.387 ± 0.003	0.327 ± 0.006
	total	0.0042 ± 0.0005	0.0840 ± 0.0017	1.491 ± 0.019	0.160 ± 0.002	0.813 ± 0.006	0.387 ± 0.004	0.328 ± 0.006
Yamato-74112	600	0.0033 ± 0.0006	0.0701 ± 0.0031	0.981 ± 0.020	0.150 ± 0.006	0.788 ± 0.011	0.395 ± 0.011	0.340 ± 0.007
(27.3 mg)	1200	0.0040 ± 0.0011	0.0748 ± 0.0035	1.204 ± 0.020	0.152 ± 0.004	0.799 ± 0.016	0.397 ± 0.009	0.343 ± 0.009
	1800	0.0041 ± 0.0007	0.0809 ± 0.0015	1.253 ± 0.016	0.160 ± 0.002	0.812 ± 0.008	0.388 ± 0.004	0.331 ± 0.005
	total	0.0040 ± 0.0008	0.0783 ± 0.0021	1.204 ± 0.018	0.157 ± 0.003	0.806 ± 0.010	0.390 ± 0.006	0.334 ± 0.006
Yamato-790521	600	0.0035 ± 0.0005	0.0700 ± 0.0028	0.989 ± 0.023	0.151 ± 0.005	0.790 ± 0.015	0.390 ± 0.008	0.337 ± 0.009
(34.2 mg)	1200	0.0041 ± 0.0020	0.0740 ± 0.0024	1.054 ± 0.020	0.151 ± 0.003	0.788 ± 0.009	0.395 ± 0.006	0.334 ± 0.007
	1800	0.0051 ± 0.0016	0.1022 ± 0.0027	1.634 ± 0.023	0.163 ± 0.003	0.819 ± 0.006	0.386 ± 0.005	0.324 ± 0.006
	total	0.0045 ± 0.0015	0.0885 ± 0.0026	1.356 ± 0.022	0.157 ± 0.003	0.805 ± 0.008	0.389 ± 0.006	0.329 ± 0.006
Yamato-791826	600	0.0044 ± 0.0043	0.0786 ± 0.0069	1.018 ± 0.027	0.152 ± 0.005	0.793 ± 0.026	0.393 ± 0.011	0.344 ± 0.017
(28.6 mg)	1200	0.0575 ± 0.0244	0.1443 ± 0.0184	1.053 ± 0.060	0.171 ± 0.009	0.942 ± 0.041	0.471 ± 0.025	0.427 ± 0.023
	1800	0.1072 ± 0.0155	0.2268 ± 0.0186	1.030 ± 0.038	0.258 ± 0.011	1.235 ± 0.063	0.431 ± 0.015	0.393 ± 0.010
	total	0.0691 ± 0.0204	0.1650 ± 0.0177	1.044 ± 0.051	0.196 ± 0.009	1.021 ± 0.046	0.454 ± 0.021	0.411 ± 0.019
Yamato-791067	600	0.0055 ± 0.0058	0.0805 ± 0.0085	1.199 ± 0.035	0.159 ± 0.015	0.819 ± 0.042	0.391 ± 0.025	0.324 ± 0.009
(32.1 mg)	1200	0.0104 ± 0.0064	0.0883 ± 0.0106	1.301 ± 0.071	0.162 ± 0.017	0.819 ± 0.039	0.371 ± 0.017	0.321 ± 0.024
	1800	0.0070 ± 0.0020	0.0823 ± 0.0026	1.611 ± 0.033	0.161 ± 0.003	0.821 ± 0.011	0.400 ± 0.009	0.339 ± 0.008
	total	0.0073 ± 0.0036	0.0831 ± 0.0053	1.470 ± 0.041	0.161 ± 0.008	0.820 ± 0.022	0.393 ± 0.014	0.333 ± 0.011
NWA869	600	0.0024 ± 0.0011	0.0737 ± 0.0041	1.119 ± 0.021	0.153 ± 0.003	0.794 ± 0.008	0.390 ± 0.007	0.340 ± 0.010
(32.4 mg)	1200	0.0041 ± 0.0037	0.0750 ± 0.0041	1.961 ± 0.132	0.153 ± 0.011	0.800 ± 0.019	0.393 ± 0.017	0.343 ± 0.016
	1800	0.0041 ± 0.0014	0.0810 ± 0.0028	1.524 ± 0.020	0.158 ± 0.002	0.815 ± 0.004	0.387 ± 0.005	0.330 ± 0.005
	total	0.0040 ± 0.0021	0.0788 ± 0.0033	1.649 ± 0.055	0.157 ± 0.005	0.809 ± 0.009	0.389 ± 0.009	0.334 ± 0.009
Sahara98222	600	0.0041 ± 0.0025	0.0707 ± 0.0023	0.992 ± 0.026	0.150 ± 0.003	0.786 ± 0.008	0.393 ± 0.009	0.340 ± 0.008
(23.4 mg)	1200	0.0049 ± 0.0028	0.0707 ± 0.0040	1.095 ± 0.028	0.157 ± 0.008	0.806 ± 0.022	0.393 ± 0.012	0.340 ± 0.012
	1800	0.0070 ± 0.0028	0.0814 ± 0.0038	1.292 ± 0.021	0.155 ± 0.006	0.808 ± 0.024	0.398 ± 0.009	0.338 ± 0.008
	total	0.0050 ± 0.0027	0.0731 ± 0.0031	1.085 ± 0.025	0.153 ± 0.005	0.796 ± 0.015	0.395 ± 0.010	0.339 ± 0.009
Willard (b)	400	0.0014 ± 0.0091	0.0837 ± 0.0153	1.126 ± 0.102	0.148 ± 0.026	0.825 ± 0.048	0.409 ± 0.038	0.335 ± 0.043
(27.0 mg)	500	0.0039 ± 0.0009	0.0722 ± 0.0021	1.017 ± 0.016	0.152 ± 0.002	0.791 ± 0.006	0.392 ± 0.005	0.336 ± 0.006
	600	0.0036 ± 0.0015	0.0756 ± 0.0025	1.060 ± 0.017	0.155 ± 0.004	0.802 ± 0.014	0.384 ± 0.006	0.336 ± 0.007
	700	0.0057 ± 0.0024	0.0800 ± 0.0063	1.153 ± 0.032	0.160 ± 0.010	0.805 ± 0.024	0.391 ± 0.009	0.331 ± 0.017
	800	0.0033 ± 0.0031	0.0798 ± 0.0062	1.241 ± 0.034	0.163 ± 0.007	0.830 ± 0.029	0.384 ± 0.006	0.336 ± 0.011
	900	0.0046 ± 0.0062	0.0768 ± 0.0054	1.343 ± 0.027	0.161 ± 0.009	0.817 ± 0.018	0.391 ± 0.010	0.336 ± 0.007
	1000	0.0054 ± 0.0025	0.0804 ± 0.0018	1.511 ± 0.043	0.161 ± 0.007	0.827 ± 0.013	0.395 ± 0.014	0.339 ± 0.011
	1100	0.0036 ± 0.0013	0.0790 ± 0.0023	1.380 ± 0.022	0.160 ± 0.005	0.816 ± 0.015	0.387 ± 0.009	0.330 ± 0.006
	1200	0.0039 ± 0.0007	0.0811 ± 0.0018	1.313 ± 0.017	0.160 ± 0.002	0.813 ± 0.007	0.387 ± 0.004	0.328 ± 0.007
	1300	0.0043 ± 0.0012	0.0818 ± 0.0015	1.092 ± 0.014	0.162 ± 0.002	0.816 ± 0.007	0.387 ± 0.005	0.327 ± 0.006
	1400	0.0037 ± 0.0005	0.0810 ± 0.0016	1.076 ± 0.015	0.162 ± 0.003	0.815 ± 0.009	0.387 ± 0.003	0.325 ± 0.005
	1600	0.0042 ± 0.0014	0.0796 ± 0.0020	1.117 ± 0.015	0.162 ± 0.002	0.812 ± 0.010	0.385 ± 0.005	0.327 ± 0.007
	1800	0.0041 ± 0.0017	0.0789 ± 0.0035	1.134 ± 0.025	0.159 ± 0.004	0.815 ± 0.007	0.393 ± 0.011	0.330 ± 0.008
	total	0.0042 ± 0.0017	0.0794 ± 0.0026	1.182 ± 0.021	0.160 ± 0.004	0.813 ± 0.012	0.388 ± 0.006	0.331 ± 0.008
Gladstone	600	0.0037 ± 0.0007	0.0754 ± 0.0016	1.068 ± 0.019	0.152 ± 0.003	0.791 ± 0.020	0.381 ± 0.005	0.328 ± 0.010
(60.8 mg)	800	0.0037 ± 0.0017	0.0747 ± 0.0063	1.266 ± 0.065	0.150 ± 0.018	0.804 ± 0.047	0.384 ± 0.030	0.334 ± 0.017
	1000	0.0057 ± 0.0015	0.0802 ± 0.0088	1.321 ± 0.042	0.155 ± 0.011	0.790 ± 0.031	0.374 ± 0.013	0.340 ± 0.020
	1200	0.0049 ± 0.0017	0.0835 ± 0.0079	1.428 ± 0.072	0.148 ± 0.012	0.784 ± 0.028	0.382 ± 0.026	0.321 ± 0.013
	1400	0.0048 ± 0.0010	0.0805 ± 0.0034	1.307 ± 0.019	0.157 ± 0.003	0.794 ± 0.022	0.384 ± 0.006	0.326 ± 0.006
	1600	0.0039 ± 0.0004	0.0782 ± 0.0023	1.079 ± 0.006	0.157 ± 0.002	0.795 ± 0.009	0.379 ± 0.004	0.323 ± 0.003
	1800	0.0040 ± 0.0003	0.0788 ± 0.0018	1.104 ± 0.009	0.156 ± 0.002	0.796 ± 0.012	0.382 ± 0.001	0.324 ± 0.003
	total	0.0046 ± 0.0012	0.0784 ± 0.0059	1.242 ± 0.040	0.154 ± 0.010	0.795 ± 0.028	0.379 ± 0.015	0.332 ± 0.013